

University of Groningen

The lung extracellular matrix protein landscape in severe early-onset and moderate chronic obstructive pulmonary disease

Joglekar, Mugdha M; Bekker, Nicolaas J; Koloko Ngassie, Maunick Lefin; Vonk, Judith M; Borghuis, Theo; Reinders-Luinge, Marjan; Bakker, Janna; Woldhuis, Roy R; Pouwels, Simon D; Melgert, Barbro N

Published in:

American Journal of Physiology - Lung Cellular and Molecular Physiology

DOI:

[10.1152/ajplung.00332.2023](https://doi.org/10.1152/ajplung.00332.2023)

IMPORTANT NOTE: You are advised to consult the publisher's version (publisher's PDF) if you wish to cite from it. Please check the document version below.

Document Version

Publisher's PDF, also known as Version of record

Publication date:

2024

[Link to publication in University of Groningen/UMCG research database](#)

Citation for published version (APA):

Joglekar, M. M., Bekker, N. J., Koloko Ngassie, M. L., Vonk, J. M., Borghuis, T., Reinders-Luinge, M., Bakker, J., Woldhuis, R. R., Pouwels, S. D., Melgert, B. N., Timens, W., Brandsma, C.-A., & Burgess, J. K. (2024). The lung extracellular matrix protein landscape in severe early-onset and moderate chronic obstructive pulmonary disease. *American Journal of Physiology - Lung Cellular and Molecular Physiology*, 327(3), L304-L318. <https://doi.org/10.1152/ajplung.00332.2023>

Copyright

Other than for strictly personal use, it is not permitted to download or to forward/distribute the text or part of it without the consent of the author(s) and/or copyright holder(s), unless the work is under an open content license (like Creative Commons).

The publication may also be distributed here under the terms of Article 25fa of the Dutch Copyright Act, indicated by the "Taverne" license. More information can be found on the University of Groningen website: <https://www.rug.nl/library/open-access/self-archiving-pure/taverne-amendment>.





Take-down policy

If you believe that this document breaches copyright please contact us providing details, and we will remove access to the work immediately and investigate your claim.

Downloaded from the University of Groningen/UMCG research database (Pure): <http://www.rug.nl/research/portal>. For technical reasons the number of authors shown on this cover page is limited to 10 maximum.

RESEARCH ARTICLE

The lung extracellular matrix protein landscape in severe early-onset and moderate chronic obstructive pulmonary disease

 **Mugdha M. Joglekar**^{1,2*}  **Nicolaas J. Bekker**^{1,2*}  **Maunick Lefin Koloko Ngassie**^{1,2,3*}
 **Judith M. Vonk**^{2,4} **Theo Borghuis**^{1,2} **Marjan Reinders-Luinge**¹ **Janna Bakker**¹  **Roy R. Woldhuis**^{1,2}
 **Simon D. Pouwels**^{1,2,5}  **Barbro N. Melgert**^{2,6}  **Wim Timens**^{1,2}  **Corry-Anke Brandsma**^{1,2*} and
 **Janette K. Burgess**^{1,2,7*}

¹University of Groningen, University Medical Center Groningen, Department of Pathology and Medical Biology, Groningen, The Netherlands; ²University of Groningen, University Medical Center Groningen, Groningen Research Institute for Asthma and COPD (GRIAC), Groningen, The Netherlands; ³Department of Anesthesiology and Perioperative Medicine, Mayo Clinic, Rochester, Minnesota, United States; ⁴University of Groningen, University Medical Center Groningen, Department of Epidemiology, Groningen, The Netherlands; ⁵University of Groningen, University Medical Center Groningen, Department of Pulmonary Diseases, Groningen, The Netherlands; ⁶University of Groningen, Department of Molecular Pharmacology, Groningen, The Netherlands; and ⁷University of Groningen, University Medical Center Groningen, Department of Biomedical Sciences, KOLFF Institute, Groningen, The Netherlands

Abstract

Extracellular matrix (ECM) remodeling has been implicated in the irreversible obstruction of airways and destruction of alveolar tissue in chronic obstructive pulmonary disease (COPD). Studies investigating differences in the lung ECM in COPD have mainly focused on some collagens and elastin, leaving an array of ECM components unexplored. We investigated the differences in the ECM landscape comparing severe-early onset (SEO)-COPD and moderate COPD to control lung tissue for collagen type I α chain 1 (COL1A1), collagen type VI α chain 1 (COL6A1); collagen type VI α chain 2 (COL6A2), collagen type XIV α chain 1 (COL14A1), fibulin 2 and 5 (FBLN2 and FBLN5), latent transforming growth factor β binding protein 4 (LTBP4), lumican (LUM), versican (VCAN), decorin (DCN), and elastin (ELN) using image analysis and statistical modeling. Percentage area and/or mean intensity of expression of LUM in the parenchyma, and COL1A1, FBLN2, LTBP4, DCN, and VCAN in the airway walls, was proportionally lower in COPD compared to controls. Lowered levels of most ECM proteins were associated with decreasing forced expiratory volume in 1 s (FEV₁) measurements, indicating a relationship with disease severity. Furthermore, we identified six unique ECM signatures where LUM and COL6A1 in parenchyma and COL1A1, FBLN5, DCN, and VCAN in airway walls appear essential in reflecting the presence and severity of COPD. These signatures emphasize the need to examine groups of proteins to represent an overall difference in the ECM landscape in COPD that are more likely to be related to functional effects than individual proteins. Our study revealed differences in the lung ECM landscape between control and COPD and between SEO and moderate COPD signifying distinct pathological processes in the different subgroups.

NEW & NOTEWORTHY Our study identified chronic obstructive pulmonary disease (COPD)-associated differences in the lung extracellular matrix (ECM) composition. We highlight the compartmental differences in the ECM landscape in different subtypes of COPD. The most prominent differences were observed for severe-early onset COPD. Moreover, we identified unique ECM signatures that describe airway walls and parenchyma providing insight into the intertwined nature and complexity of ECM changes in COPD that together drive ECM remodeling and may contribute to disease pathogenesis.

collagen; COPD; extracellular matrix; ECM signatures; image analysis

INTRODUCTION

Chronic obstructive pulmonary disease (COPD) is a lung disease with increasing prevalence globally (1). The pathogenesis of COPD has been largely attributed to prolonged

exposure to cigarette smoke, air pollution, or occupational pollutants in combination with genetic predisposition. These factors initiate a process that causes a decline in lung function, which is evaluated clinically by measuring the forced expiratory volume in 1 s (FEV₁) (2). Based on

*M. M. Joglekar, N. J. Bekker, and M. L. Koloko Ngassie contributed equally to this work. C.-A. Brandsma and J. K. Burgess contributed equally to this work.

Correspondence: J. K. Burgess (j.k.burgess@umcg.nl).

Submitted 31 October 2023 / Revised 3 May 2024 / Accepted 12 June 2024



FEV₁ measurements, the Global Initiative for Chronic Obstructive Lung Diseases (GOLD) has classified COPD into four stages: COPD stage I, II, III, and IV (3).

COPD patients present with several phenotypes, reflecting the heterogeneity of the disease, including chronic bronchitis in the airways and emphysema in the alveoli distal to terminal bronchioles. Deposition and remodeling of the extracellular matrix (ECM) in the airway wall contributes to irreversible airway wall thickening. Conversely, emphysema is characterized by the destruction of alveolar tissue causing loosening and ultimately loss of alveolar attachments and elastic recoil. The ECM is a three-dimensional network of proteins, proteoglycans, and glycosaminoglycans that provides structural support, including tensile strength and elasticity to the lung and essential biochemical and biophysical cues to cells (4). Several studies, often with conflicting results, have highlighted differences in ECM content in COPD as previously reviewed (5, 6).

Several studies have drawn parallels between physiological lung aging and COPD, as these processes share multiple hallmarks including dysregulated ECM remodeling. Thus “accelerated aging” is often considered one of the main features of COPD (7–9). Apart from the most common phenotypes of COPD (bronchitis and emphysema), the severity and age of onset of the disease can define certain subgroups of patients. Historically, COPD is considered a disease of the elderly, predominantly male smokers. However, it is now clear that a subgroup of patients, with a high prevalence among women, develop very severe COPD at a much earlier age (often younger than 55 yr) and this group is referred to as severe early onset (SEO)-COPD patients (8, 10, 11).

Our group recently reported age-associated ECM differences in human lung tissue using a combination of transcriptomic and proteomic analyses (12). Seven ECM and ECM-associated proteins including collagen type I α chain 1 (COL1A1), collagen type VI α chain 1 (COL6A1); collagen type VI α chain 2 (COL6A2), collagen type XIV α chain 1 (COL14A1), fibulin 2 (FBLN2), latent transforming growth factor β binding protein 4 (LTBP4), and lumican (LUM) were found to have higher expression with increasing age at gene and protein levels in healthy subjects. Immunohistochemical studies further illustrated higher levels of COL1A1, COL6A2, COL14A1, and LUM in different lung compartments with age. We hypothesized that the proteins involved in the aging processes of the lung also play a key role in the pathology of COPD. In the present study, we aimed to investigate whether these seven age-related proteins showed similar differences in COPD lung tissue and whether the degree of these differences was related to disease severity (i.e., FEV₁) and COPD subgroups, i.e., SEO-COPD and moderate COPD. Additionally, other important matrix proteins including fibulin 5 (FBLN5), decorin (DCN), versican (VCAN), and elastin (ELN) that are of known biological relevance in the pathology of COPD (13–15) were also investigated to identify differences in the ECM landscape between control, SEO-COPD, and moderate COPD lungs. Finally, statistical modeling was performed on the combined set of ECM and ECM-associated proteins to define COPD ECM signatures in the different compartments of the lung, specific for COPD, SEO-COPD and moderate COPD.

MATERIALS AND METHODS

Ethics Statements

The study was conducted in accordance with the Research Code of the University Medical Center Groningen (UMCG), as stated on <https://umcgresearch.org/w/research-code-umcg>, as well as national ethical and professional guidelines Code of Conduct for Health Research (<https://www.coreon.org/wp-content/uploads/2023/06/Code-of-Conduct-for-Health-Research-2022.pdf>). The use of leftover lung tissue in this study was not subject to the Medical Research Human Subjects Act in the Netherlands, as confirmed by a statement of the Medical Ethical Committee of the University Medical Center Groningen, and therefore exempt from consent according to national laws (Dutch laws: Medical Treatment Agreement Act (WGBO) art 458/GDPR art 9/AVG art 24). All donor material and clinical information were deidentified before experimental procedures, blinding any identifiable information to the investigators.

Subjects

COPD and control human lung tissues were obtained from material left over following lung transplants and tumor resection surgeries at the University Medical Center Groningen (Groningen, The Netherlands). In the latter, only lung tissue sections distant from the resected tumor that appeared normal upon macroscopic and histological evaluation were accepted for use. This study was part of the HOLLAND (Histopathology of Lung Aging and COPD) cohort and the included nondiseased control subjects are a subset of the donors previously studied by Koloko et al. (12). The donors were selected based on the following inclusion criteria:

- 1) SEO-COPD patients: percent predicted FEV₁ (FEV₁% pred) <40%, FEV₁/forced vital capacity (FVC) <70%, and age \leq 55 yr at the time of lung transplant surgery, ex-smokers (10, 11, 16, 17);
- 2) Non-COPD control subjects (matched with SEO-COPD): FEV₁/FVC >70%, age <65 yr at the time of surgery, ex-smokers;
- 3) Moderate COPD patients: FEV₁%pred = 40–80%, FEV₁/FVC <70%, age >65 yr at the time of surgery, ex-smokers; and
- 4) Non-COPD control subjects (matched with moderate COPD): FEV₁/FVC >70%, age >65 yr at the time of surgery, ex-smokers.

For patients where both pre- and post-bronchodilator FEV₁, FVC, and FEV₁/FVC measurements were available, the best measurement was chosen for inclusion. The tissue used in the current study is material left over following diagnostic procedures and was procured by technicians who were independent of the investigators involved in the staining and analyses of the current study.

Immunohistochemistry

Briefly, lung tissue obtained from COPD ($n = 26$) and control ($n = 18$) donors was formalin fixed and paraffin embedded (FFPE) and cut into 6- μ m sections. Before staining, the sections were deparaffinized and rehydrated. The full methodology for staining COL1A1, COL6A1, COL6A2, COL14A1, FBLN2, LTBP4, and LUM has been previously described (12).

For FBLN5, VCAN, ELN, and DCN sections were treated with Tris/EDTA buffer (10 mM, pH 9) for antigen retrieval. The sections were washed with PBS and endogenous peroxidase activity was blocked using hydrogen peroxidase (0.3%) for 30 min at room temperature. Following PBS washes, primary antibodies (Table 1) diluted in 1% BSA/PBS for FBLN5 (1:8,000), DCN (1:1,500), VCAN (1:200), and ELN (1:400) were added to the respective sections for 1 h at room temperature. After the incubation period, the sections were washed and horseradish peroxidase-conjugated secondary antibody rabbit anti-mouse (1:100, P0260, Dako, Glostrup, Denmark) was added to FBLN5, DCN, and VCAN staining and goat anti-rabbit (1:100, P0448, Dako) was added to ELN sections in 1% BSA-PBS containing 1% human serum. Similarly, tertiary antibody goat anti-rabbit (1:100, P0448, Dako) was used to stain FBLN5, DCN, and VCAN sections while rabbit anti-goat (1:100, P0449, Dako) was used for ELN in 1% BSA-PBS containing 1% human serum for after washing away of the secondary antibodies. Negative controls (no primary antibody) were also included. Finally, positive staining in the sections was visualized with Vector NovaRED substrate (SK-4800, Vector Laboratories, Burlington, Canada). Hematoxylin was used to counterstain these sections. All sections used for examination of a given protein were stained at the same time. The sections were dehydrated and mounted and scanned at $\times 40$ using a digital slide scanner Hamamatsu Nanozoomer 2.0HT (Hamamatsu Photonic K.K., Hamamatsu, Japan). An Aperio ImageScope (v12.4.6.5003, Leica Biosystems, Wetzlar, Germany) was used to view these digital images.

Image Analysis

The expression and localization of proteins in COPD compared to control donors were investigated in the airways and

Table 1. Primary antibodies used for staining different proteins

Protein	Primary Antibody
COL1A1	Monoclonal mouse, anti-human, ab88147, 1:400, Abcam, IgG3
COL6A1	Polyclonal rabbit, anti-human, NB120-6588, 1:3,200, Novus Biologicals, IgG
COL6A2	Monoclonal rabbit, anti-human, ab180855, 1:12,500, Abcam, IgG
COL14A1	Polyclonal rabbit, anti-human, HPA023781, 1:100, Atlas Antibodies, IgG
FBLN2	Polyclonal rabbit, anti-human, HPA001934, 1:400, Atlas Antibodies, IgG
FBLN5	Monoclonal mouse anti-Fibulin 5/DANCE antibody 1G6A4, Novus Biologicals, IgG1
LTBP4	Polyclonal rabbit, anti-human, ab222844, 1:400, Abcam, IgG
LUM	Monoclonal rabbit, anti-human, ab168348, 1:12,500, Abcam, IgG
DCN	Monoclonal mouse anti-dermatan sulfate proteoglycan antibody 6B6, Seikagaku, IgG1
VCAN	Monoclonal mouse anti-versican antibody 2B1, Seikagaku, IgG1
ELN	Polyclonal rabbit anti-elastin antibody CL55011AP, Cedarlane Labs, IgG

COL1A1, collagen type I α chain 1; COL6A1, collagen type VI α chain 1; COL6A2, collagen type VI α chain 2; COL14A1, collagen type XIV α chain 1; DCN, decorin; ELN, elastin; FBLN2, fibulin 2; FBLN5, fibulin 5; IgG, immunoglobulin G; LTBP4, latent transforming growth factor β binding protein 4; LUM, lumican; VCAN, versican.

parenchymal regions of the lung tissue, as described previously (12). Individual compartments were extracted from tissue scans using an Aperio ImageScope. Depending on the donor, up to a maximum of 10 airways (< 2 mm in diameter) were extracted from each section. After extraction, specific areas of interest including parenchyma and airway walls were further isolated using Adobe Photoshop 2023 (Adobe Inc., San Jose, CA). The protocol followed for image analysis is illustrated in Fig. 1. Briefly, the color deconvolution plugin developed by Landini et al (18) was used to extract the red (NovaRed) and blue (hematoxylin) pixels from each image. The optical density vectors were optimized using the protocol described by Ruifrok et al. (19) and a vector was developed to measure the values of each pixel. Total area of the tissue section was determined by converting each image to an 8-bit grayscale. The threshold feature of Fiji (20) quantified total number of pixels and number of pixels positively stained. The thresholds were selected, using ten representative images, manually by ensuring that all the regions positive for that color were included and the negative areas remained excluded. The selected thresholds were verified in negative controls of each protein. The percentage area of tissue stained for the ECM protein was calculated using the formula in Eq. 1. The mean intensity of staining was calculated using a protocol described by Nguyen (21). The pixel intensities of our images ranged from 0–255 in Fiji, where 0 is the darkest and 255 is the lightest shade. As intensities are inversely proportional to the degree of coloration, reciprocal intensities were calculated, and the mean intensity was obtained using the formula in Eq. 2. Data sorting and calculations were performed using R software (version 4.2.3).

$$\text{Percentage area} = \frac{\text{Number of pixels positive for NovaRed}}{\text{Number of pixels in total tissue}} \times 100 \quad (1)$$

$$\text{Mean intensity} = 255 - \frac{\text{Sum of intensities of pixels positive for NovaRed}}{\text{Total number of pixels positive for NovaRed}} \quad (2)$$

Statistical Analysis

Donor characteristics including age, sex, pack-years, FEV₁%pred, and FEV₁/FVC were compared between subgroups of COPD and matched control group using Mann-Whitney *U* tests. Percentage area and mean intensity of proteins that were not normally distributed were log (natural) transformed, and these transformed values were used for further analysis. The differences in percentage area and mean intensity of protein levels in COPD and control lung tissue were examined using linear regression analysis for parenchyma and linear mixed-effects regression analysis with a random effect on intercept per subject for airway walls. These models were also used to compare subgroups of COPD (moderate COPD and SEO-COPD) to their respective matched controls. Regression coefficients with the 95% confidence intervals were plotted. Furthermore, linear and linear mixed models were also used to investigate associations between age (corrected for disease status) or FEV₁%pred measurements

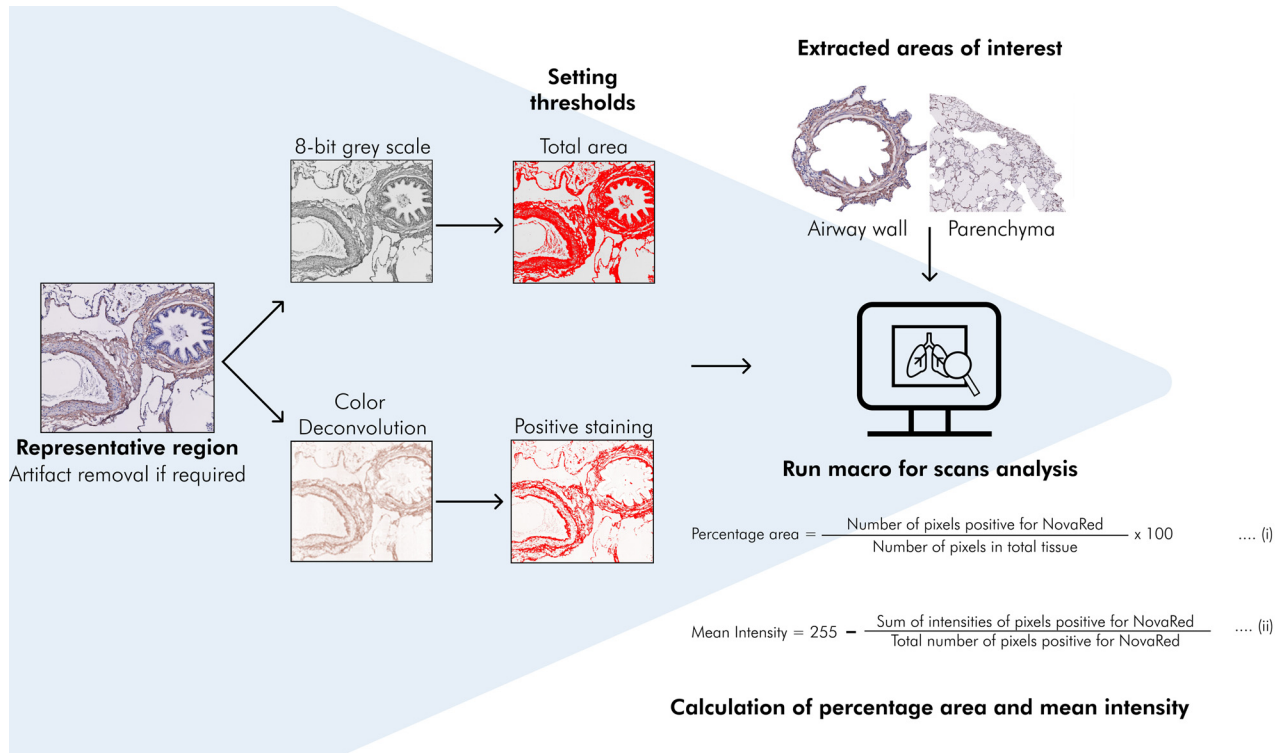


Figure 1. An overview of the methods used for image analysis. Representative regions were extracted from 10 donors. The representative regions were converted to an 8-bit grayscale image or color deconvoluted to extract red channels that were further utilized to set thresholds for total area of the tissue and positively stained area, respectively. All extracted regions were analyzed using macros and formulas (i) and (ii) to derive percentage area and mean intensity values. [Image created with Figma and Flaticon]

and percentage area or mean intensity of each protein in parenchyma and airway walls, respectively.

Principal component analysis (PCA) with varimax rotation was used to identify unique ECM and ECM-associated protein signatures in COPD. Z scores of raw protein values (non-transformed or log transformed) were used as input, and “n” components were extracted that cumulatively explained at least 80% of the variance. The component scores were saved for further analysis. Component scores of COPD and control donors were compared per component using linear and linear mixed modeling for parenchyma and airway wall, respectively. The comparisons of component scores between subgroups of COPD (SEO-COPD or moderate COPD) to all controls were performed using linear and linear mixed modeling, corrected for age. P value of <0.05 was considered significant. Data were

analyzed using IBM SPSS version 28.0.1.0(142). Scatter and forest plots were created in GraphPad Prism version 8.0.0.

RESULTS

Patient Characteristics

The clinical parameters of donors included in this study are summarized in Table 2. All subjects included in this study were ex-smokers. The COPD group (n = 26) comprised moderate COPD (n = 14) and SEO-COPD (n = 12). For analyses that investigated the effect of COPD subgroups, the control group (n = 18) was divided into older control (n = 9) subjects matched in age and sex to moderate COPD and younger control subjects (n = 9) matched in age and sex to SEO-COPD (n = 9).

Table 2. Characteristics of donors included in this study

	Younger Controls	SEO-COPD	Older Controls	Moderate COPD
Age in years (median, range)	55.0 (43.0–62.0)	51.5 (47.0– 55.0)	74.0 (67.0–81.0)	72.0 (67.0– 81.0)
Sex (female/male)	6/3	8/4	3/6	2/12
Pack-years (median, range)	15.0 (1.5–40.0)	25.0 (6.0–54.0)	35.0 (5.0–52.5)	41.0 (10.0–65.0)
FEV ₁ %pred (median %predicted, range)	103.6 (85.0–127.0)	19.3 (14.9– 23.6)†	91.5 (75.8–133.0)	62.0 (49.7–75.4)‡
FEV ₁ /FVC (median, range)	76.0 (69.0*–86.6)	27.3 (20.5– 68.0)†	72.0 (69.0–86.1)	60.8 (43.6– 67.9)‡

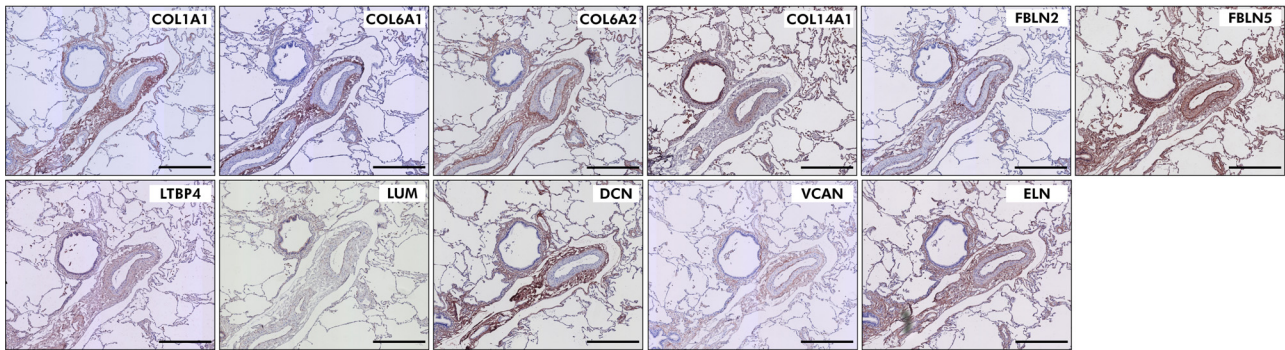
SEO-COPD (n = 12) and moderate COPD (n = 14) were matched in terms of age, sex, and smoking status to respective younger and older control groups. P < 0.05 was considered significant. COPD, chronic obstructive pulmonary disease; FEV₁%pred, forced expiratory volume in 1 s %predicted; FVC, forced vital capacity; SEO-COPD, severe early-onset COPD. *2 controls had an FEV₁/forced vital capacity (FVC) of 69% due to a relatively high FVC in combination with normal FEV₁. †P < 0.0005 and ‡P < 0.0005, comparison between SEO-COPD and younger controls and moderate COPD and older controls, respectively.

Localization of ECM and ECM-Associated Proteins in Lung Tissue

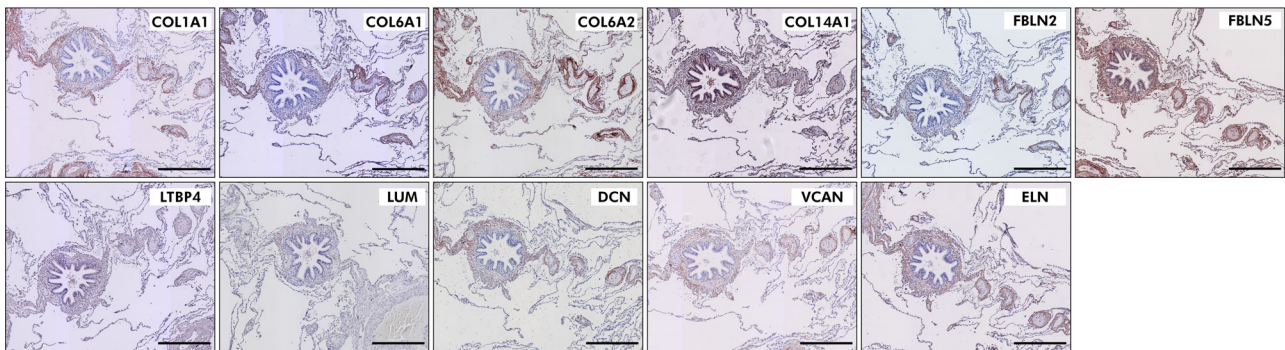
The immunohistochemically stained lung tissues were examined for the localization of proteins in COPD and control lung tissue. An overview of some examples of staining of COL1A1, COL6A1, COL6A2, COL14A1, FBLN2, FBLN5, LTBP4, LUM, DCN, VCAN, and ELN for each group are depicted in Fig. 2, and available as enlarged images in Supplemental Fig. S1. The localization of each staining has been summarized in Table 3, and the heterogeneity in staining patterns within each group has been

noted in Supplemental Tables S1, S2, and S3. The distribution of staining and heterogeneity of localization across control, moderate, and SEO-COPD tissues was similar for most proteins examined in this study, with the exception of potential differences in VCAN and ELN. For VCAN and ELN, strong staining was more often seen in controls, whereas in patients with COPD, the pattern was more heterogeneous with a bell-shaped distribution with more patients having moderate and fewer with weak or strong staining. Briefly, all 11 proteins were detected in the parenchyma and COL14A1, LTBP4, and LUM staining was also detected in the epithelial layer. Within the airway

Control



SEO-COPD



Moderate COPD

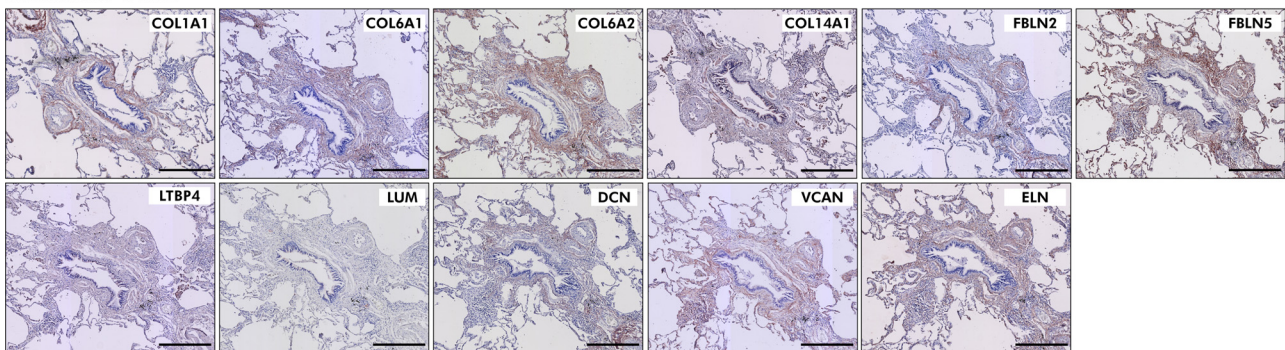


Figure 2. Localization of ECM and ECM-associated proteins in control, SEO, and moderate COPD parenchyma and airway walls. FFPE lung tissue sections from control and COPD donors were stained using immunohistochemistry for ECM and ECM-associated proteins with specific signals being detected with Nova red (red) and counterstained with hematoxylin (blue). Sections were scanned at $\times 40$ magnification using a digital slide scanner. Scale bar = 400 μ m. Images are representative of protein detection patterns seen in control donors ($n = 18$), SEO-COPD ($n = 12$), and moderate COPD ($n = 14$). COL1A1, collagen type I α chain 1; COL6A1, collagen type VI α chain 1; COL6A2, collagen type VI α chain 2; COL14A1, collagen type XIV α chain 1; COPD, chronic obstructive pulmonary disease; DCN, decorin; ECM, extracellular matrix; ELN, elastin; FBLN2, fibulin 2; FBLN5, fibulin 5; FFPE, formalin fixed paraffin embedded; LTBP4, latent transforming growth factor β binding protein 4; LUM, lumican; SEO-COPD, severe early-onset COPD patients; VCAN, versican.

Table 3. Localization of ECM and ECM-associated proteins in lung tissue

ECM Protein	Parenchyma	Epithelial Layer	Airway Wall		
			SM	AA	ASM
COL1A1	+	—	+	+	—/+
COL6A1	+	—	+	+	+
COL6A2	+	—	+	+	+
COL14A1	+	+	+	+	+
FBLN2	+	—	+	+	—
FBLN5	+	—	+	+	—
LTBP4	+	+	+	+	+
LUM	+	+	+	+	+
DCN	+	—	—/+	+	—
VCAN	+	—	+	+	—
ELN	+	—	+	+	—

An overview of positively stained areas in lung tissue. —, No staining; +, positive staining; AA, airway adventitia; ASM, airway smooth muscle; COL1A1, collagen type I α chain 1; COL6A1, collagen type VI α chain 1; COL6A2, collagen type VI α chain 2; COL14A1, collagen type XIV α chain 1; DCN, decorin; ECM, extracellular matrix; ELN, elastin; FBLN2, fibulin 2; FBLN5, fibulin 5; LTBP4, latent transforming growth factor β binding protein 4; LUM, lumican; VCAN, versican; SM, submucosa.

wall, all proteins were detected in the airway adventitia and submucosa apart from DCN, which was donor dependent. In the vicinity of the airway smooth muscle, COL6A1, COL6A2, COL14A1, LTBP4, and LUM were detected along with COL1A1 in some donors.

Distribution of ECM and ECM-Associated Proteins in COPD Lung Tissue Compared to Matched Controls

The distribution of ECM and ECM-associated proteins that have been previously associated with age-related changes, or with COPD pathology, was investigated using image analysis and statistical modeling. Percentage area and mean intensity of positive pixels for each ECM protein were compared between COPD and matched controls, followed by subgroup analysis for SEO and moderate COPD compared to their matched controls.

Differences in lung parenchyma: lower proportional levels of LUM in COPD and SEO-COPD.

When comparing the staining of ECM and ECM-associated proteins in lung parenchyma between all COPD patients and all controls, we observed a lower proportional percentage area of the tissue that was positive for LUM ($P = 0.010$) and a lower mean intensity of the positive LUM pixels ($P = 0.022$) in COPD compared to control tissue (Fig. 3, A and D). Subgroup analysis demonstrated that this lower LUM percentage area was most apparent in SEO-COPD ($P = 0.012$; Fig. 3B). There were no significant differences observed for the other ECM proteins between COPD and control, nor in the SEO or moderate COPD subgroup analysis (Fig. 3, C, E, and F). The percentage area or mean intensity of expression of some ECM proteins was significantly associated with age (see Supplemental Fig. S2), as also reported in our previous publication (12). However, this did not alter the differences between COPD and control because these cohorts were age-matched.

Differences in the airway walls: lower proportional levels of COL1A1, FBLN2, LTBP4, DCN, and VCAN in COPD and SEO-COPD.

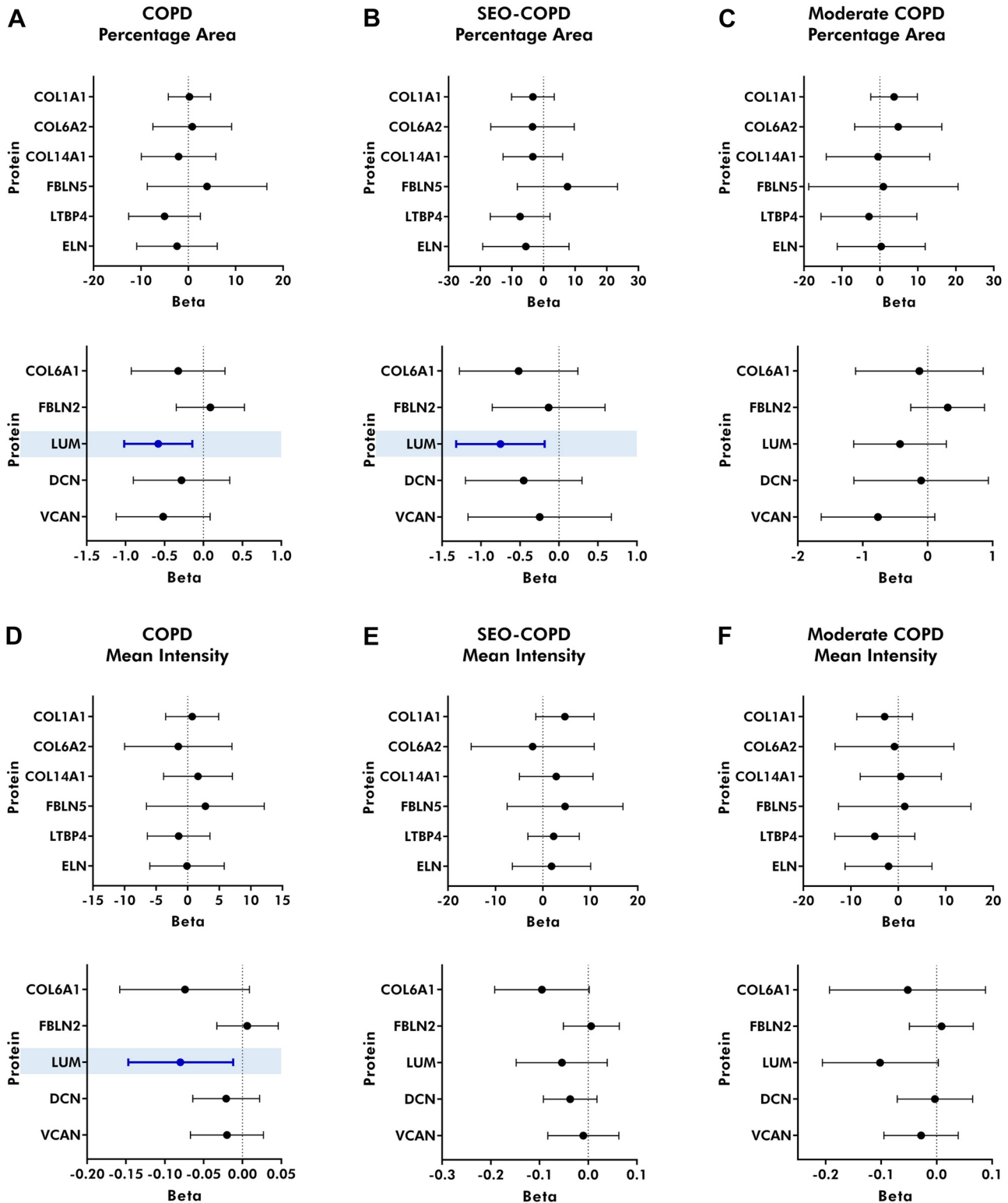
When comparing the staining of ECM and ECM-associated proteins in airway walls between COPD and controls, several proteins had proportionally lower percentage area and mean intensity of expression in COPD compared to control airway walls. In the COPD group, the percentage area of DCN ($P = 0.045$) and mean intensities of COL1A1 ($P = 0.016$) were proportionally lower compared to the control group (Fig. 4, A and D). Furthermore, subgroup analysis demonstrated proportionally lower percentage areas of COL1A1 ($P = 8.3 \times 10^{-5}$), FBLN2 ($P = 0.014$), and LTBP4 ($P = 0.016$) and mean intensities of COL1A1 ($p = 0.013$), LTBP4 ($P = 0.020$), and VCAN ($P = 0.031$) in the airway walls of the SEO-COPD donors compared to matched controls (Fig. 4, B and E). Similar to the parenchyma, no differences were observed when comparing moderate COPD donors to their matched controls (Fig. 4, C and F). The percentage area and mean intensity of expression of certain ECM proteins were significantly associated with age (see Fig. S3) as also reported in our previous publication (12); however, this did not alter the differences between COPD and control because these cohorts were age matched.

Differences in the Levels of ECM and ECM-Associated Proteins in the Parenchyma and Airway Walls Are Associated with FEV₁

Correlations between percentage area and mean intensity of ECM and ECM-associated proteins with lung function (FEV₁%pred) were evaluated to investigate any relationships between proportionally lower ECM protein levels with lung function (Supplemental Table S4). In the parenchyma, the percentage area of LUM and mean intensity of COL6A1 were positively associated with FEV₁%pred when all donors were included. Subgroup analysis of COPD donors for parenchyma did not result in any associations between FEV₁%pred and ECM proteins. However, the percentage area of FBLN2 and DCN and mean intensity of VCAN and ELN were positively associated with control donors. In contrast, the percentage area of COL1A1, FBLN2, LTBP4, and VCAN and mean intensity of COL1A1 and VCAN were positively associated with FEV₁%pred in the airways when all donors were grouped. Interestingly, on subgroup analysis of COPD donors for airways, percentage area and mean intensity of COL1A1 were positively associated with FEV₁%pred, while percentage area and mean intensity of FBLN5 were negatively associated with FEV₁%pred. In control donors exclusively, the mean intensity of ELN was positively associated with FEV₁%pred.

Identification of Novel Parenchymal and Airway Wall ECM Signatures for COPD and COPD Subgroups Using Percentage Area of Protein Expression

Having analyzed the localization, distribution, and degree of expression of each protein individually, we were also interested to explore whether there were any multicomponent identifying patterns within our data set that reflected the ECM differences related to the COPD status of the patients. To explore these possible patterns, we used PCA to



identify unique groupings of the proteins, which initially examined the percentage area positive staining for each protein. PCA analysis resulted in four and six components in the parenchyma and airway wall, respectively, each consisting of a different set of ECM proteins, to explain at least 80% of the total variance (as seen in the scree plot) (Fig. 5, A and B).

When comparing the component scores for each component between COPD and control in the parenchyma, we identified a significantly lower score for the fourth component in COPD compared to controls, indicating that the combination of ECM proteins in this component reflects a parenchymal ECM signature for COPD (Fig. 5C). The percentage area of

LUM, LTBP4, DCN, COL6A1, and ELN was the highest contributor of variance in this component (Table 4). Subsequent subgroup analysis showed that this component was also significantly lower in SEO compared to controls (Supplemental Fig. S4A), supporting our earlier observations of the differences in the parenchymal regions being mainly in the SEO-COPD patients. Thus these five proteins together provide a unique ECM signature for differences in COPD and SEO-COPD parenchyma as compared to control.

In the airway walls, component scores of the COPD cohort were observed to be lower in the second component (Fig. 5D). The percentage area of COL6A1, DCN, FBLN5, VCAN, and COL14A1 was the highest contributor to component 2, thereby uniquely describing COPD airway walls (Table 5). Subgroup analysis indicated that the moderate group drove the differences observed in the second component (Supplemental Fig. S4B). Additionally, SEO-COPD donors had higher scores in component three compared to controls (Supplemental Fig. S4B). Thus COL6A1, DCN, FBLN5, VCAN, and COL14A1 form a unique ECM signature for COPD airway walls, and the combined pattern of COL1A1, FBLN5, and COL14A1 describes the difference between moderate and SEO-COPD.

While these signatures are based on measurements of percentage area, mean intensities were also used to identify unique ECM signatures (Supplemental Fig. S5 and Tables S5 and S6) for COPD status in parenchyma and airway walls. Mean intensities of LUM, COL6A1, LTBP4, COL6A2, and VCAN together formed an ECM signature for COPD parenchyma, while COL1A1, FBLN5, and COL6A2 described COPD airways.

COPD-Associated Differences in the Lung ECM

We have summarized the differences seen in the landscape of ECM in the lung parenchyma and airway walls in COPD and the subgroups (SEO and moderate) in Fig. 6. Only those proteins that were observed to have significant associations with COPD or its subgroups have been indicated.

DISCUSSION

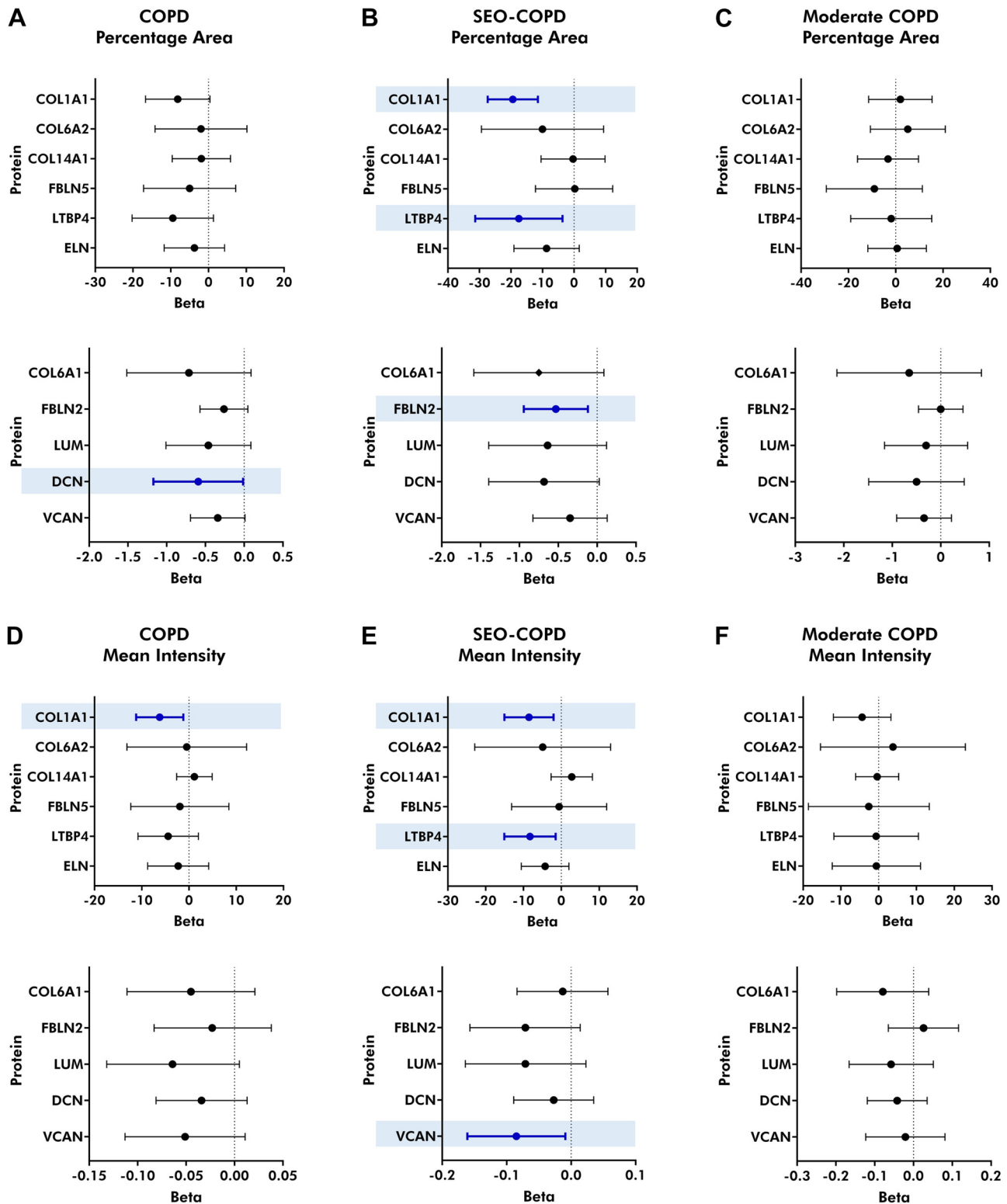
Our study provides an elaborate investigation of 11 ECM and ECM-associated proteins in COPD lung tissue. Important novelties of this study are the combination of the comparison between airway walls and lung parenchyma, the inclusion of different COPD subgroups, characterization of proteins that have not yet been studied in COPD lung tissue, and the investigation of mean intensity, in addition to percentage tissue area of expression of each protein. Overall, the SEO-COPD group showed the most ECM differences in composition

compared to controls. Notably, we generated unique ECM signatures that described moderate and SEO-COPD independently, potentially reflecting differing tissue remodeling processes that are part of the disease pathogenesis in these COPD subtypes.

ECM dysregulation has been postulated as a common hallmark of aging and COPD (8). Previously our group identified specific profiles of age-associated genes and a negative interaction between age and the presence of COPD for several ECM-related genes, indicating a different association of age with COPD and control (22). Our follow-up study focused on ECM differences with normal aging and revealed higher expression of COL1A1, COL6A1, COL6A2, FBLN2, LTBP4, and LUM at both gene and protein levels in aging lungs of control patients with normal lung function and no history of COPD, pulmonary fibrosis, or asthma (12). Additionally, immunohistochemical analysis showed higher levels of COL6A2 in the airway walls and COL6A2 and COL1A1 in the parenchyma with aging lungs in control subjects. This age-related ECM profile in control patients did not overlap with the ECM signature reported for COPD in the present study, where we observed proportionally lower ECM and ECM-associated protein percentage area and/or mean intensity in COPD. This suggests that the observed ECM profile in COPD is different from age-related ECM differences in non-COPD controls and can be either driven by the pathobiology of COPD or represent a form of abnormal aging in COPD. Notably, parenchyma in both aging and COPD is affected by emphysema; however, changes in the airway wall structures are less comparable between the two as airway thickening is not as apparent in aging lungs.

ECM differences in COPD have long been an area of interest (23). However, results from different studies are often conflicting. In the current study, we identified more COPD-associated differences in the airway walls compared to the parenchyma. It is important to note that, as a result of emphysematous loss of the lung parenchyma, tissue obtained from COPD patients in the more severe stages only allows us to examine the parenchyma and airways that are still remaining in the lung. It is quite likely that the ECM composition of the lost tissue was also aberrant; however, this cannot be characterized *ex vivo*. Moreover, we report proportional differences in the ECM content in the airway walls in COPD compared to control tissue. Proportional differences do not necessarily indicate that there is less total ECM content in the airway wall but rather that the proportion of the different ECM components is changing. Thus there may be an absolute increase in other ECM proteins in the airways, due to the fibrotic nature of the changes observed in COPD, that have

Figure 3. Forest plots of regression coefficients for percentage area and mean intensity of ECM and ECM-associated proteins in the parenchyma of COPD, SEO-COPD, and moderate COPD compared to their respective control groups. ECM proteins in FFPE tissue sections from controls ($n = 18$), SEO-COPD ($n = 12$), and moderate COPD ($n = 14$) were detected using immunohistochemistry. Parenchyma was isolated and analyzed for percentage positive tissue area and mean intensity of positive pixels of expression for each protein. All 44 donors were available for analysis of COL1A1, COL6A2, FBLN2, LTBP4, LUM, DCN, VCAN, and ELN, while for COL6A1, COL14A1, and FBLN5 43 donors were available. For each protein, regression coefficients (\pm 95% confidence interval) were obtained following linear regression, and $P < 0.05$ was considered significant. Non-transformed variables are plotted first, followed by log transformed variables. The differences in ECM and ECM-associated proteins in COPD tissue were compared to control in terms of percentage area (A–C) and mean intensity (D–F) of positively stained pixels. Dark blue-colored bars in light blue-colored boxes highlight significant differences. COL1A1, collagen type I α chain 1; COL6A1, collagen type VI α chain 1; COL6A2, collagen type VI α chain 2; COL14A1, collagen type XIV α chain 1; COPD, chronic obstructive pulmonary disease; DCN, decorin; ECM, extracellular matrix; ELN, elastin; FBLN2, fibulin 2; FBLN5, fibulin 5; LTBP4, latent transforming growth factor β binding protein 4; FFPE, formalin fixed paraffin embedded; LUM, lumican; SEO-COPD, severe early-onset COPD; VCAN, versican.



not been captured in this study. It is thus important to assess more ECM proteins, such as collagen III, as a relative increase in COL3 over COL1 has been previously demonstrated in COPD tissue (24). In parenchyma and airway walls alike, protein levels did not differ between the moderate COPD group and their matched controls. The ECM

profiles in the moderate COPD patients, who were older compared to SEO-COPD patients, also did not resemble the differences in ECM as noted previously in aging lungs. It is clear from the present study that the pathogenesis of moderate and SEO-COPD in terms of ECM landscape is different and capturing data in SEO-COPD patients earlier

would help understand the similarities in disease mechanisms between the two subgroups. Unfortunately, SEO-COPD patients are often diagnosed at the stage where their symptoms are quite severe and the tissue is collected at the time of lung transplantation; thus early stage data are scarce.

Collagens are the most abundant proteins in the lung ECM. Fibrillar collagens (type I and III) are crucial in maintaining the structural integrity and organization of the lung tissue by forming three-dimensional networks and providing mechanical strength (25). Less fractional area and volume fraction of collagen type I in COPD lungs have previously been reported in small airways by Annoni et al. (26) and bronchiolar tissue by Hogg et al. (24), respectively. These findings align with the lower proportion of COL1A1 in the airway walls of COPD patients observed in our study. However, neither of these previous studies compared the differences between COPD severities, while we observed that SEO-COPD donors dominantly contribute to the lower proportion of COL1A1 in COPD within the airway wall. In parenchyma, Eurlings et al. (27) demonstrated a higher percentage area of collagen (type I/II/III) in the remaining alveolar walls of COPD subjects, which increased with disease severity, whereas we did not observe differences in the proportion of COL1A1 in the parenchyma. Eurlings et al. examined older COPD stage IV patients, compared to the relatively younger SEO-COPD donors in our study, providing a possible explanation for the inconsistent findings between both studies.

Another category of ECM proteins is proteoglycans, and we have investigated LUM, DCN, and VCAN. LUM, DCN, and VCAN play a role in various cellular functions, bind to growth factors and chemokines, and regulate fibrillogenesis (28–32). The fractional area of LUM in COPD lung tissue compared to controls has been previously reported by Annoni et al. (26) who did not observe any differences between COPD donors and controls. In contrast to the study of Annoni et al, we showed a lower percentage area of LUM in the parenchymal region of COPD patients, in particular in SEO-COPD. Annoni et al. also reported lower VCAN fractional area in parenchyma in COPD and Merrilees et al. (33) observed that the alveolar walls of COPD patients showed stronger VCAN staining than control donors. In our study, a lower mean intensity of VCAN was observed in the airway walls of SEO-COPD patients. Consistent with our finding of a lower proportional percentage area of DCN in COPD airway walls, a previous study reported lower DCN staining in the airway adventitia of severe emphysematous tissue, while only a few donors with mild emphysema displayed lower staining (15). However, in our current study, we did not

observe an association between DCN staining intensity and disease severity. The loss of proteoglycans can not only directly alter cellular responses (34) but also affect the structural integrity of lung tissue due to the resulting disorganized ECM components and modified mechanical properties such as lung elasticity and alveolar stability (35).

FBLNs are calcium-binding glycoproteins that bind to other ECM aggregates and stabilize them. They bind to the basement membrane and also elastic fibers (36). In our previous study, we observed a positive correlation between the percentage area of FBLN2 and the mean intensity of COL1A1 in the parenchyma with age in control never-smokers (12). Interestingly, in COPD lungs, a lower percentage area of FBLN2 was accompanied by a lower percentage area and mean intensity of COL1A1 in SEO-COPD donors in airway walls. Despite both being observational studies, these results incite further investigation into the FBLN2/COL1A1 axis as a possible regulatory mechanism for the stabilization of collagen fibers around the airways (26, 27, 37). An earlier study from our group reported higher total levels of FBLN5 in COPD tissue homogenates compared to controls using Western blot, along with colocalization of FBLN5 with ELN fibers using immunohistochemical staining in lung tissue (38).

Next to assessing all ECM differences separately, it is also relevant to study the patterns in ECM differences. Together these differences form the ECM landscape in COPD and may contribute to the change in mechanical properties of the lung such as loss of elastic recoil and airflow obstruction of COPD airways. This is supported by the correlation of the expression of several of these proteins with FEV₁ measurements. Moreover, a recent study reported softer emphysematous precision-cut lung slices with decreased stiffness compared to healthy controls (39). With the help of computation network modeling, they attributed this reduced stiffness to ECM remodeling of the septal wall along with structural deterioration of the lung. In the current study, we identified ECM signatures that represent groups of proteins the characteristics of which describe COPD and the different severities of COPD. It is clear from the various results obtained in our study that LUM, COL6A1, and LTBP4 are important in describing COPD parenchyma ECM characteristics. Similarly, COL1A1, COL14A1, FBLN5, DCN, and VCAN appear essential in describing characteristic factors in ECM remodeling in the airway walls in COPD (Fig. 6).

Collagen type I and III are major components of the lung ECM. However, several supporting ECM and ECM-associated proteins are required to maintain the structural integrity and function of collagens. Per our knowledge, the expression of

Figure 4. Forest plots of regression coefficients for percentage area and mean intensity of ECM and ECM-associated proteins in the airway walls of COPD, SEO-COPD, and moderate COPD compared to their respective control groups. ECM proteins present in FFPE tissue sections from controls ($n = 18$), SEO-COPD ($n = 12$), and moderate COPD ($n = 14$) were detected using immunohistochemistry. Airway walls were isolated and analyzed for percentage area and mean intensity of expression for each protein. The number of airway walls available for the analysis for each protein were COL1A1 ($n = 155$), COL6A1 ($n = 150$), COL6A2 ($n = 149$), COL14A1 ($n = 152$), FBLN2 ($n = 158$), FBLN5 ($n = 173$), LTBP4 ($n = 163$), LUM ($n = 158$), DCN ($n = 156$), VCAN ($n = 165$), and ELN ($n = 158$). For each protein, regression coefficients ($\pm 95\%$ confidence interval) were obtained following linear regression, and $P < 0.05$ was considered significant. Non-transformed variables are plotted first, followed by log transformed variables. The differences in ECM and ECM-associated proteins in COPD tissue were compared to control in terms of percentage area (A–C) and mean intensity (D–F) of positively stained pixels. Dark blue-colored bars in light blue-colored boxes highlight significant differences. COL1A1, collagen type I α chain 1; COL6A1, collagen type VI α chain 1; COL6A2, collagen type VI α chain 2; COL14A1, collagen type XIV α chain 1; COPD, chronic obstructive pulmonary disease; DCN, decorin; ECM, extracellular matrix; ELN, elastin; FFPE, formalin fixed paraffin embedded; FBLN2, fibulin 2; FBLN5, fibulin 5; LTBP4, latent transforming growth factor β binding protein 4; LUM, lumican; SEO-COPD, severe early-onset COPD; VCAN, versican.

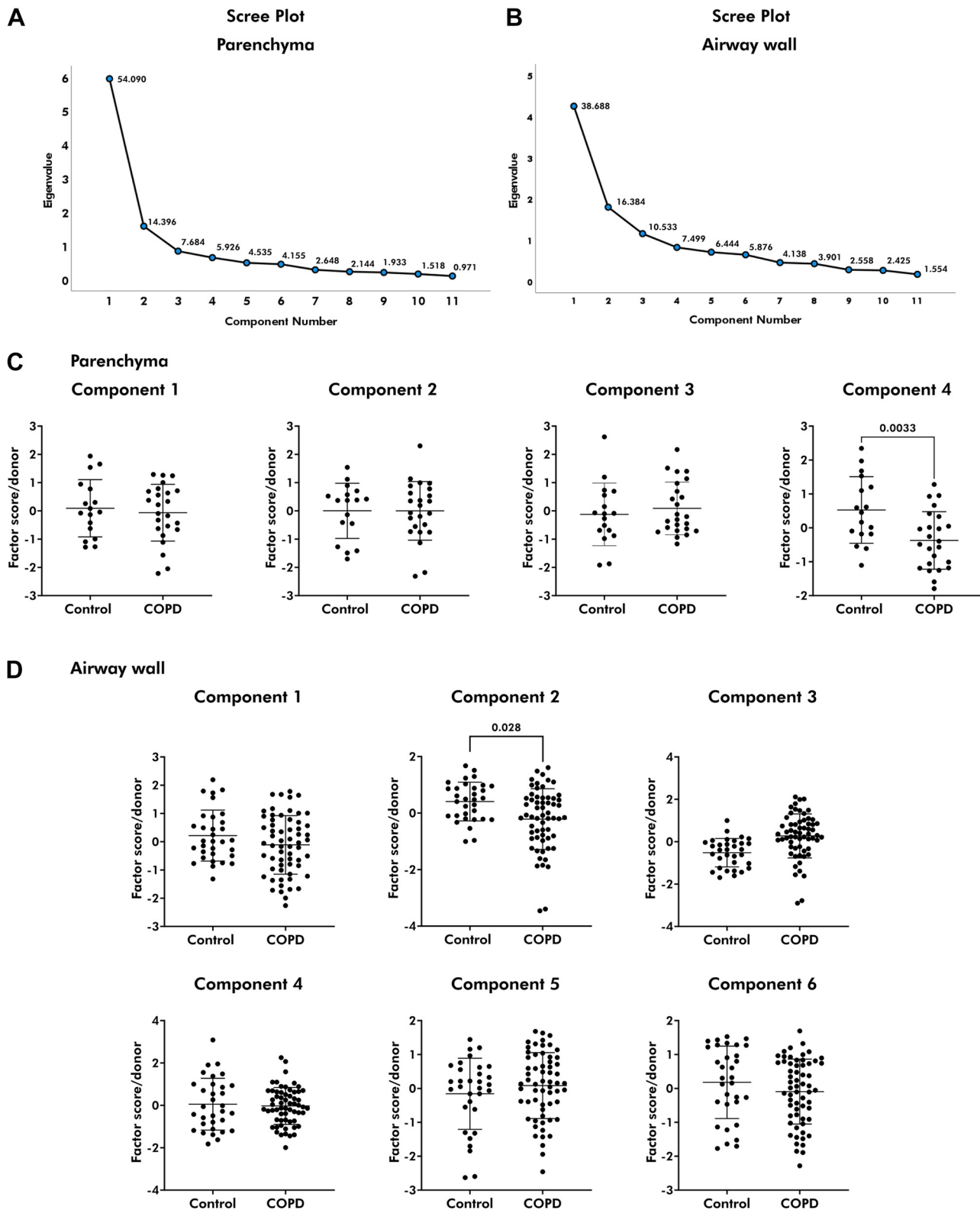


Figure 5. Identifying unique extracellular matrix (ECM) signatures for chronic obstructive pulmonary disease (COPD) using protein expression in terms of percentage area. Principal component analysis (PCA) was performed for percentage area of proteins in parenchyma and airway walls. PCA eliminates an entire donor or airway in the absence of measurement for even one protein out of the 11, leaving fewer donors for parenchyma ($n = 41$) and airway walls ($n = 93$) in these analyses. A and B: 4 (A) and 6 (B) components, respectively, explained at least 80% of the total variance in parenchyma and airway wall as shown in the scree plot. The component scores obtained following PCA were compared using linear and linear mixed models to investigate the differences between the control and COPD groups, and the mean \pm SD has been plotted. C: in the parenchymal region, the patterns in proteins between COPD and control were different in component 4 ($P = 0.003$). D: differences in the patterns of proteins between control and COPD donors were noted in component 2 ($P = 0.028$) in the airway walls.

Table 4. Rotated component matrix for principal component analysis of percentage tissue areas positive of ECM and ECM-associated proteins in the parenchyma

Rotated Component Matrix: Parenchyma				
	1	2	3	4*
VCAN	0.814	0.308		
FBLN2	0.802		0.376	
ELN	0.751		0.399	0.308
COL14A1		0.918		
FBLN5	0.439	0.791		
COL6A1	0.373	0.662	0.311	0.333
LTBP4	0.532	0.533		0.468
DCN	0.345	0.489	0.483	0.387
COL1A1	0.398		0.839	
COL6A2		0.472	0.637	
LUM				0.917

Four components explained at least 80% of the total variance. The loadings of each ECM and ECM-associated protein as obtained as a result of the principal component were tabulated. The loadings represent the correlations between the proteins and the component. COL1A1, collagen type I α chain 1; COL6A1, collagen type VI α chain 1; COL6A2, collagen type VI α chain 2; COL14A1, collagen type XIV α chain 1; DCN, decorin; ECM, extracellular matrix; ELN, elastin; FBLN2, fibulin 2; FBLN5, fibulin 5; LTBP4, latent transforming growth factor β binding protein 4; LUM, lumican; VCAN, versican. * $P < 0.005$, comparison between chronic obstructive pulmonary disease donors and controls. Only loadings $>|0.3|$ are shown.

LTBPs in lung tissue has not been studied in the context of COPD. LTBPs not only regulate the signaling of transforming growth factor β (TGF- β) but also mediate elastogenesis (40, 41). LTBP4 binds to TGF- β 1 and guides its deposition into the ECM after cellular secretion. Thus less proportional presence of LTBP4 may result in lower TGF- β 1 activation and diminished elastogenesis. Another consequence of decreased TGF- β -Smad pathway activation is the attenuation of DCN in COPD lungs and hence disruption of collagen assembly (42). Moreover, abnormal loosening of collagen fibers might make ELN susceptible to destruction. A study in adult rats reported

Table 5. Rotated component matrix for principal component analysis of percentage tissue areas positive of ECM and ECM-associated proteins in the airway walls

Rotated Component Matrix: Airway Walls						
	1	2*	3†	4	5	6
ELN	0.918					
FBLN2	0.762				0.400	
VCAN	0.633	0.482		0.300		
COL6A1		0.873				
DCN	0.496	0.663				
COL1A1			−0.823			
FBLN5		0.557	0.710			
LTBP4	0.471			0.788		
COL14A1		0.336	0.367	0.698		
COL6A2					0.893	
LUM						0.977

Six components explained at least 80% of the total variance. The loadings of each ECM and ECM-associated protein as obtained as a result of the principal component analysis were tabulated. The loadings represent the correlations between the proteins and the component. COL1A1, collagen type I α chain 1; COL6A1, collagen type VI α chain 1; COL6A2, collagen type VI α chain 2; COL14A1, collagen type XIV α chain 1; COPD, chronic obstructive pulmonary disease; DCN, decorin; ECM, extracellular matrix; ELN, elastin; FBLN2, fibulin 2; FBLN5, fibulin 5; LTBP4, latent transforming growth factor β binding protein 4; LUM, lumican; VCAN, versican; SEO-COPD, severe early-onset COPD. * $P < 0.05$, comparison between COPD donors and controls. † $P < 0.05$, comparison between SEO-COPD, moderate, and control donors corrected for age. Only loadings $>|0.3|$ are shown.

that the turnover rate of collagens is 10–15% per day (43); however, the formation of ELN fibers declines with age and is almost absent in adulthood (44). Additionally, relatively lower protein levels of factors regulating elastogenesis, such as LTBP4 and FBLN2 in the current study, potentially hamper ELN repair. In our study, however, we did not observe a difference in the percentage area or mean intensity of ELN. Several studies have shown a reduction of ELN fibers in airways and parenchyma; however, no differences were noted between

Parenchyma			Airway wall		
		Percentage area	Mean intensity	Percentage area	Mean intensity
Staining	COPD	LUM ↓	LUM ↓	DCN ↓	COL1A1 ↓
	SEO-COPD	LUM ↓		COL1A1 ↓ FBLN2 ↓ LTBP4 ↓	COL1A1 ↓ LTBP4 ↓ VCAN ↓
	Moderate COPD				
FEV1 associations	All donors	LUM ↑	COL6A1 ↑	COL1A1 ↑ FBLN2 ↑ LTBP4 ↑ VCAN ↑	COL1A1 ↑ VCAN ↑
	COPD donors			COL1A1 ↑ FBLN5 ↓	COL1A1 ↑ FBLN5 ↓
	Control donors	FBLN2 ↑ DCN ↑	VCAN ↑ ELN ↑		ELN ↑
ECM Signatures	COPD	LUM, LTBP4, DCN, COL6A1, ELN ↓	LUM, COL6A1, LTBP4, COL6A2, VCAN ↓	COL6A1, DCN, FBLN5, VCAN, COL14A1 ↓	COL1A1, FBLN5, COL6A2 ↓
	SEO-COPD	LUM, LTBP4, DCN, COL6A1, ELN ↓	COL1A1, LTBP4, ELN ↑	COL1A1, FBLN5, COL14A1 ↑	
	Moderate COPD			COL6A1, DCN, FBLN5, VCAN, COL14A1 ↓	

Figure 6. COPD-associated differences in lung ECM. ECM differences noted in the different analyses throughout this study have been summarized here. In the staining and ECM signatures, red or blue arrows indicate higher or lower proportional levels or component scores in COPD, respectively, while they denote positive or negative associations with FEV₁, respectively. COL1A1, type I collagen α chain 1; COL6A1, type VI collagen α chain 1; COL6A2, type VI collagen α chain 2; COL14A1, type XIV collagen α chain 1; COPD, chronic obstructive pulmonary disease; DCN, decorin; ECM, extracellular matrix; ELN, elastin; FEV₁, forced expiratory volume in 1 second; FBLN2, fibulin 2; FBLN5, fibulin 5; LTBP4, latent transforming growth factor β binding protein 4; LUM, lumican; SEO-COPD, severe early-onset COPD; VCAN, versican. [Image created with Figma.]

different stages of COPD (26, 37). Notably, the unique signatures identified for airway walls and parenchyma suggest compartmental differences during reparative processes. Among proteoglycans, LUM was proportionally lower in the parenchyma while DCN and VCAN were lower in the airway walls. This could indicate that LUM is more closely associated with collagen assembly in the parenchyma, while DCN and VCAN are more critical in the airway walls. While most proteins appear in either the parenchymal or airway wall signature alone, COL6 appears in both. It is localized near the basement membrane region forming a meshwork between the basement membrane and the interstitial matrix. The role of COL6 in mechanical regulation of the lung has previously been postulated (45). Its presence in both signatures suggests a key role for COL6 in the overall COPD pathology. Collagen type XIV is found in regions of high mechanical strength. It is well-known that the mechanical properties of airway walls in COPD, including fibrosis and loss of elastic recoil, are altered (46). Thus, it is not surprising that we observed COL6A1, COL6A2, and COL14A1 localized in the airway smooth muscle region and these proteins appear important in our airway wall signatures. Our results suggest that COL6 and COL14A1 likely are important contributors to airway wall pathology that leads to the obstruction and ultimately the collapse of airways in COPD.

A limitation of this study is the small number of patients included in the subgroup analysis. The heterogeneity of COPD, patient inclusion criteria, and analysis methods may account for the variability in the data seen among these studies. Despite these limitations, we reported robust findings. Our results not only support the investigation of pathways involving ECM and ECM-associated proteins involved in this study but also are a reminder that disease pathogenesis is not driven and characterized by a single protein but rather by complex interactions between groups of proteins.

In conclusion, we identified COPD-associated differences in the lung ECM composition. The differences in the ECM landscape may affect the integrity of the structure and function of the lung tissue compartments. Our study has identified proteins, including LUM in the parenchyma and COL1A1, LTBP4, FBLN2, and VCAN in the airway walls that have not previously been associated with the SEO-COPD subtypes. Moreover, we report unique ECM signatures for parenchyma and airway walls associated with disease and COPD severity. The identified proteins may contribute to the establishment and maintenance of disease pathology in SEO-COPD patients and thus provides leads for future studies.

DATA AVAILABILITY

Data will be made available upon reasonable request.

SUPPLEMENTAL MATERIAL

Supplementary Figs. S1–S5 and Supplemental Tables S1–S6: <https://doi.org/10.6084/m9.figshare.25726917>.

ACKNOWLEDGMENTS

Preprint is available at <https://doi.org/10.1101/2023.10.20.562391>. Graphical abstract was created with Figma (<https://www.figma.com/>) and Flaticon (<https://www.flaticon.com/>) (with appropriate licenses).

GRANTS

M.M.J. acknowledges support from the Graduate School of Medical Sciences, University of Groningen. N.J.B. is funded by the Public-Private Partnerships (PPP) allowance by Health Holland (Life Sciences & Health) and the University Medical Center Groningen (UMCG). This collaboration project is co-financed by the Ministry of Economic Affairs and Climate Policy by means of the PPP allowance made available by the Top Sector Life Sciences & Health to stimulate PPPs. M.L.K.N. receives support from Abel Tasman Talent Program Fellowship in association with the Healthy Aging Alliance from the UMCG. R.R.W. acknowledges support from the Lung Foundation Netherlands (Longfonds 5.2.21.006). C.-A.B. receives from Nederlandse Organisatie voor Wetenschappelijk Onderzoek (NWO; Aspasia 015.015.044). J.K.B. acknowledges support from the NWO (Aspasia 015.013.010).

DISCLOSURES

W.T. receives consulting fees from Bristol-Myers-Squibb, Astellas, and Merck Sharp Dohme, all fees to UMCG. He is also a member of the Council for Research and Innovation of the Federation of Medical Specialists. C.-A.B. received unrestricted research grants from Genentech. J.K.B. receives unrestricted research funds from Boehringer Ingelheim. None of the other authors has any conflicts of interest, financial or otherwise, to disclose.

AUTHOR CONTRIBUTIONS

M.M.J., N.J.B., M.L.K.N., W.T., C.-A.B., and J.K.B. conceived and designed research; N.J.B., M.L.K.N., T.B., M.R.-L., and J.B. performed experiments; M.M.J., N.J.B., M.L.K.N., J.M.V., and T.B. analyzed data; M.M.J., N.J.B., M.L.K.N., J.M.V., W.T., C.-A.B., and J.K.B. interpreted results of experiments; M.M.J. and M.L.K.N. prepared figures; M.M.J., N.J.B., M.L.K.N., J.M.V., C.-A.B., and J.K.B., and drafted manuscript; M.M.J., N.J.B., M.L.K.N., J.M.V., T.B., M.R.-L., J.B., R.R.W., S.D.P., B.N.M., W.T., C.-A.B., and J.K.B. edited and revised manuscript; M.M.J., N.J.B., M.L.K.N., J.M.V., T.B., M.R.-L., J.B., R.R.W., S.D.P., B.N.M., W.T., C.-A.B., and J.K.B., approved final version of manuscript.

REFERENCES

- Adeloye D, Song P, Zhu Y, Campbell H, Sheikh A, Rudan I; **NIHR RESPIRE Global Respiratory Health Unit**. Global, regional, and national prevalence of, and risk factors for, chronic obstructive pulmonary disease (COPD) in 2019: a systematic review and modelling analysis. *Lancet Respir Med* 10: 447–458, 2022. doi:10.1016/S2213-2600(21)00511-7.
- Lange P, Celli B, Agustí A, Boje Jensen G, Divo M, Faner R, Guerra S, Marott JL, Martinez FD, Martinez-Camblor P, Meek P, Owen CA, Petersen H, Pinto-Plata V, Schnohr P, Sood A, Soriano JB, Tesfayiz Y, Vestbo J. Lung-function trajectories leading to chronic obstructive pulmonary disease. *N Engl J Med* 373: 111–122, 2015. doi:10.1056/NEJMoa1411532.
- Agustí A, Celli BR, Criner GJ, Halpin D, Anzueto A, Barnes P, Bourbeau J, Han MK, Martinez FJ, Montes de Oca M, Mortimer K, Papi A, Pavord I, Roche N, Salvi S, Sin DD, Singh D, Stockley R, López Varela MV, Wedzicha JA, Vogelmeier CF. Global Initiative for Chronic Obstructive Lung Disease 2023 report: GOLD executive summary. *Eur Respir J* 61: 2300239, 2023. doi:10.1183/13993003.00239-2023.
- Burgess JK, Harmsen MC. Chronic lung diseases: entangled in extracellular matrix. *Eur Respir Rev* 31: 210202, 2022. doi:10.1183/16000617.0202-2021.

5. Hoffman ET, Uhl FE, Asarian L, Deng B, Becker C, Uriarte JJ, Downs I, Young B, Weiss DJ. Regional and disease specific human lung extracellular matrix composition. *Biomaterials* 293: 121960, 2023. doi:10.1016/j.biomaterials.2022.121960.
6. Joglekar MM, Nizamoglu M, Fan Y, Nemani SS, Weckmann M, Pouwels SD, Heijink IH, Melgert BN, Pillay J, Burgess JK. Highway to heal: influence of altered extracellular matrix on infiltrating immune cells during acute and chronic lung diseases. *Front Pharmacol* 13: 995051, 2022. doi:10.3389/fphar.2022.995051.
7. Agustí A, Hogg JC. Update on the pathogenesis of chronic obstructive pulmonary disease. *N Engl J Med* 381: 1248–1256, 2019. doi:10.1056/NEJMra1900475.
8. Brandsma CA, De Vries M, Costa R, Woldhuis RR, Königshoff M, Timens W. Lung ageing and COPD: is there a role for ageing in abnormal tissue repair? *Eur Respir Rev* 26: 170073, 2017. doi:10.1183/16000617.0073-2017.
9. Mercado N, Ito K, Barnes PJ. Accelerated ageing of the lung in COPD: new concepts. *Thorax* 70: 482–489, 2015. doi:10.1136/thoraxjnl-2014-206084.
10. Woldhuis RR, De Vries M, Timens W, Van Den Berge M, Demaria M, Oliver BGG, Heijink IH, Brandsma CA. Link between increased cellular senescence and extracellular matrix changes in COPD. *Am J Physiol Lung Cell Mol Physiol* 319: L48–L60, 2020. doi:10.1152/ajplung.00028.2020.
11. Silverman EK, Weiss ST, Drazen JM, Chapman HA, Carey V, Campbell EJ, Denish P, Silverman RA, Celedon JC, Reilly JJ, Ginns LC, Speizer FE. Gender-related differences in severe, early-onset chronic obstructive pulmonary disease. *Am J Respir Crit Care Med* 162: 2152–2158, 2000. doi:10.1164/ajrccm.162.6.2003112.
12. Koloko Ngassie ML, De Vries M, Borghuis T, Timens W, Sin DD, Nickle D, Joubert P, Horvatovich P, Marko-Varga G, Teske JJ, Vonk JM, Gosens R, Prakash YS, Burgess JK, Brandsma CA. Age-associated differences in the human lung extracellular matrix. *Am J Physiol Lung Cell Mol Physiol* 324: L799–L814, 2023. doi:10.1152/ajplung.00334.2022.
13. Brandsma CA, Van Den Berge M, Postma D, Timens W. Fibulin-5 as a potential therapeutic target in COPD. *Expert Opin Ther Targets* 20: 1031–1033, 2016. doi:10.1517/14728222.2016.1164696.
14. Turino GM, Ma S, Lin YY, Cantor JO, Luisetti M. Matrix elastin: a promising biomarker for chronic obstructive pulmonary disease. *Am J Respir Crit Care Med* 184: 637–641, 2011. doi:10.1164/rccm.201103-0450PP.
15. van Straaten JF, Coers W, Noordhoek JA, Huitema S, Flipsen JT, Kauffman HF, Timens W, Postma DS. Proteoglycan changes in the extracellular matrix of lung tissue from patients with pulmonary emphysema. *Mod Pathol* 12: 697–705, 1999.
16. Foreman MG, Zhang L, Murphy J, Hansel NN, Make B, Hokanson JE, Washko G, Regan EA, Crapo JD, Silverman EK, DeMeo DL; COPD Gene Investigators. Early-onset chronic obstructive pulmonary disease is associated with female sex, maternal factors, and African American race in the COPD Gene Study. *Am J Respir Crit Care Med* 184: 414–420, 2011. doi:10.1164/rccm.201011-1928OC.
17. Stanley SE, Chen JJ, Podlevsky JD, Alder JK, Hansel NN, Mathias RA, Qi X, Rafaels NM, Wise RA, Silverman EK, Barnes KC, Armanios M. Telomerase mutations in smokers with severe emphysema. *J Clin Invest* 125: 563–570, 2015. doi:10.1172/JCI78554.
18. Landini G, Martinelli G, Piccinini F. Colour deconvolution: stain unmixing in histological imaging. *Bioinformatics* 37: 1485–1487, 2021. doi:10.1093/bioinformatics/btaa847.
19. Ruifrok AC, Johnston DA. Quantification of histochemical staining by color deconvolution. *Anal Quant Cytol Histol* 23: 291–299, 2001.
20. Schindelin J, Arganda-Carreras I, Frise E, Kaynig V, Longair M, Pietzsch T, Preibisch S, Rueden C, Saalfeld S, Schmid B, Tinevez JY, White DJ, Hartenstein V, Eliceiri K, Tomancak P, Cardona A. Fiji: an open-source platform for biological-image analysis. *Nat Methods* 9: 676–682, 2012. doi:10.1038/nmeth.2019.
21. Nguyen D. Quantifying chromogen intensity in immunohistochemistry via reciprocal intensity. *Protoc Exch* 2: e, 2013. doi:10.1038/protex.2013.097.
22. De Vries M, Faiz A, Woldhuis RR, Postma DS, De Jong TV, Sin DD, Bossé Y, Nickle DC, Guryev V, Timens W, Van Den Berge M, Brandsma CA. Lung tissue gene-expression signature for the ageing lung in COPD. *Thorax* 73: 609–617, 2018. doi:10.1136/thoraxjnl-2017-210074.
23. Jones RL, Noble PB, Elliot JG, James AL. Airway remodelling in COPD: it's not asthma! *Respirology* 21: 1347–1356, 2016. doi:10.1111/resp.12841.
24. Hogg JC, McDonough JE, Gosselink JV, Hayashi S. What drives the peripheral lung-remodeling process in chronic obstructive pulmonary disease? *Proc Am Thorac Soc* 6: 668–672, 2009. doi:10.1513/pats.200907-079DP.
25. Mereness JA, Mariani TJ. The critical role of collagen VI in lung development and chronic lung disease. *Matrix Biol Plus* 10: 100058, 2021. doi:10.1016/j.mbplus.2021.100058.
26. Annoni R, Lanças T, Yukimatsu Tanigawa R, De Medeiros Matsushita M, De Moraes Fernezan S, Bruno A, Fernando Ferraz Da Silva L, Roughley PJ, Battaglia S, Dolhnikoff M, Hiemstra PS, Sterk PJ, Rabe KF, Mauad T. Extracellular matrix composition in COPD. *Eur Respir J* 40: 1362–1373, 2012. doi:10.1183/09031936.00192611.
27. Eurlings IM, Dentener MA, Cleutjens JPM, Peutz CJ, Rohde GG, Wouters EF, Reynaert NL. Similar matrix alterations in alveolar and small airway walls of COPD patients. *BMC Pulm Med* 14: 90, 2014. doi:10.1186/1471-2466-14-90.
28. Dolhnikoff M, Morin J, Roughley PJ, Ludwig MS. Expression of lumican in human lungs. *Am J Respir Cell Mol Biol* 19: 582–587, 1998. doi:10.1165/ajrcmb.19.4.2979.
29. Giatagana EM, Berdiaki A, Tsatsakis A, Tzanakakis GN, Nikitovic D. Lumican in carcinogenesis-revisited. *Biomolecules* 11: 1319, 2021. doi:10.3390/biom11091319.
30. Nikitovic D, Katonis P, Tsatsakis A, Karamanos NK, Tzanakakis GN. Lumican, a small leucine-rich proteoglycan. *IUBMB Life* 60: 818–823, 2008. doi:10.1002/iub.131.
31. Hwang CT, Halper J. Proteoglycans and diseases of soft tissues. *Adv Exp Med Biol* 1348: 127–138, 2021. doi:10.1007/978-3-030-80614-9_5.
32. Andersson-Sjöland A, Hallgren O, Rolandsson S, Weitoft M, Tykesson E, Larsson-Callerfelt AK, Rydell-Törmänen K, Bjerner L, Malmström A, Karlsson JC, Westergren-Thorsson G. Versican in inflammation and tissue remodeling: the impact on lung disorders. *Glycobiology* 25: 243–251, 2015. doi:10.1093/glycob/cwv120.
33. Merrilees MJ, Ching PS, Beaumont B, Hinek A, Wight TN, Black PN. Changes in elastin, elastin binding protein and versican in alveoli in chronic obstructive pulmonary disease. *Respir Res* 9: 41, 2008. doi:10.1186/1465-9921-9-41.
34. Dong Y, Zhong J, Dong L. The role of decorin in autoimmune and inflammatory diseases. *J Immunol Res* 2022: 1283383, 2022. doi:10.1155/2022/1283383.
35. Cavalcante FSA, Ito S, Brewer K, Sakai H, Alencar AM, Almeida MP, Andrade JS Jr, Majumdar A, Ingenito EP, Suki B. Mechanical interactions between collagen and proteoglycans: implications for the stability of lung tissue. *J Appl Physiol (1985)* 98: 672–679, 2005. doi:10.1152/jappphysiol.00619.2004.
36. Hanada K, Sasaki T. Expression and purification of recombinant fibulins in mammalian cells. *Methods Cell Biol* 143: 247–259, 2018. doi:10.1016/bs.mcb.2017.08.014.
37. Black PN, Ching PST, Beaumont B, Ranasinghe S, Taylor G, Merrilees MJ. Changes in elastic fibres in the small airways and alveoli in COPD. *Eur Respir J* 31: 998–1004, 2008. doi:10.1183/09031936.00017207.
38. Brandsma CA, Van Den Berge M, Postma DS, Jonker MR, Brouwer S, Paré PD, Sin DD, Bossé Y, Laviolette M, Karjalainen J, Fehrmann RSN, Nickle DC, Hao K, Spanjer AIR, Timens W, Franke L. A large lung gene expression study identifying fibulin-5 as a novel player in tissue repair in COPD. *Thorax* 70: 21–32, 2015. doi:10.1136/thoraxjnl-2014-205091.
39. Kim JH, Schaible N, Hall JK, Bartolák-Suki E, Deng Y, Herrmann J, Sonnenberg A, Behrsing HP, Lutchen KR, Krishnan R, Suki B. Multiscale stiffness of human emphysematous precision cut lung slices. *Sci Adv* 9: eadf2535, 2023. doi:10.1126/sciadv.adf2535.
40. Su CT, Urban Z. LTBP4 in health and disease. *Genes (Basel)* 12: 795, 2021. doi:10.3390/genes12060795.
41. Dabovic B, Chen Y, Choi J, Vassallo M, Dietz HC, Ramirez F, Von Melchner H, Davis EC, Rifkin DB. Dual functions for LTBP in lung development: LTBP-4 independently modulates elastogenesis and TGF- β activity. *J Cell Physiol* 219: 14–22, 2009. doi:10.1002/jcp.21643.

42. **Zandvoort A, Postma DS, Jonker MR, Noordhoek JA, Vos JTWM, van der Geld YM, Timens W.** Altered expression of the Smad signalling pathway: implications for COPD pathogenesis. *Eur Respir J* 28: 533–541, 2006. doi:[10.1183/09031936.06.00078405](https://doi.org/10.1183/09031936.06.00078405).
43. **McAnulty RJ, Laurent GJ.** Collagen synthesis and degradation in vivo. evidence for rapid rates of collagen turnover with extensive degradation of newly synthesized collagen in tissues of the adult rat. *Coll Relat Res* 7: 93–104, 1987. doi:[10.1016/s0174-173x\(87\)80001-8](https://doi.org/10.1016/s0174-173x(87)80001-8).
44. **Wagenseil JE, Mecham RP.** Vascular extracellular matrix and arterial mechanics. *Physiol Rev* 89: 957–989, 2009. doi:[10.1152/physrev.00041.2008](https://doi.org/10.1152/physrev.00041.2008).
45. **Dassah M, Almeida D, Hahn R, Bonaldo P, Worgall S, Hajjar KA.** Annexin A2 mediates secretion of collagen VI, pulmonary elasticity and apoptosis of bronchial epithelial cells. *J Cell Sci* 127: 828–844, 2014. doi:[10.1242/jcs.137802](https://doi.org/10.1242/jcs.137802).
46. **Bidan CM, Veldsink AC, Meurs H, Gosens R.** Airway and extracellular matrix mechanics in COPD. *Front Physiol* 6: 346, 2015. doi:[10.3389/fphys.2015.00346](https://doi.org/10.3389/fphys.2015.00346).